

INFORMATION TO USERS

This material was produced from a microfilm copy of the original document. While the most advanced technological means to photograph and reproduce this document have been used, the quality is heavily dependent upon the quality of the original submitted.

The following explanation of techniques is provided to help you understand markings or patterns which may appear on this reproduction.

1. The sign or "target" for pages apparently lacking from the document photographed is "Missing Page(s)". If it was possible to obtain the missing page(s) or section, they are spliced into the film along with adjacent pages. This may have necessitated cutting thru an image and duplicating adjacent pages to insure you complete continuity.
2. When an image on the film is obliterated with a large round black mark, it is an indication that the photographer suspected that the copy may have moved during exposure and thus cause a blurred image. You will find a good image of the page in the adjacent frame.
3. When a map, drawing or chart, etc., was part of the material being photographed the photographer followed a definite method in "sectioning" the material. It is customary to begin photoing at the upper left hand corner of a large sheet and to continue photoing from left to right in equal sections with a small overlap. If necessary, sectioning is continued again — beginning below the first row and continuing on until complete.
4. The majority of users indicate that the textual content is of greatest value, however, a somewhat higher quality reproduction could be made from "photographs" if essential to the understanding of the dissertation. Silver prints of "photographs" may be ordered at additional charge by writing the Order Department, giving the catalog number, title, author and specific pages you wish reproduced.
5. PLEASE NOTE: Some pages may have indistinct print. Filmed as received.

University Microfilms International

300 North Zeeb Road
Ann Arbor, Michigan 48106 USA
St. John's Road, Tyler's Green
High Wycombe, Bucks, England HP10 8HR

77-18,723

CHERWIN, Mark Gregory, 1950-
PART I: DISSOCIATION KINETICS OF MAGNESIUM
AMINOCARBOXYLATE COMPLEXES. PART II: KINETICS
OF THE POTASSIUM FERRATE OXIDATION OF
CERTAIN NITROGEN-CONTAINING COMPOUNDS,
AND THE APPLICATION OF POTASSIUM FERRATE TO
THE DETERMINATION OF CHEMICAL OXYGEN DEMAND.

The University of Nebraska - Lincoln,
Ph.D., 1977

Xerox University Microfilms, Ann Arbor, Michigan 48106

77-18,723

CHERWIN, Mark Gregory, 1950-

Chemistry, analytical

Xerox University Microfilms, Ann Arbor, Michigan 48106

PART I

DISSOCIATION KINETICS OF
MAGNESIUM AMINOCARBOXYLATE COMPLEXES

PART II

KINETICS OF THE POTASSIUM FERRATE OXIDATION OF
CERTAIN NITROGEN-CONTAINING COMPOUNDS,
AND THE APPLICATION OF POTASSIUM FERRATE TO
THE DETERMINATION OF CHEMICAL OXYGEN DEMAND

by

Mark G. Cherwin

A DISSERTATION

Presented to the Faculty of
The Graduate College in the University of Nebraska
In Partial Fulfillment of Requirements
For the Degree of Doctor of Philosophy
Department of Chemistry

Under the Supervision of Associate Professor James D. Carr

Lincoln, Nebraska

December, 1976

TITLE

Part I - Dissociation Kinetics of Magnesium Aminocarboxylate Complexes;
Part II - Kinetics of the Potassium Ferrate Oxidation of Certain
Nitrogen-containing Compounds, and the Application of Potassium Ferrate
To the Determination of Chemical Oxygen Demand

BY

Mark G. Cherwin

APPROVED

DATE

James D. Carr	12 - 16 - 76
Robert C. Larson	12 - 16 - 76
Michael L. Gross	12 - 16 - 76
Robert S. Marianelli	12 - 16 - 76

SUPERVISORY COMMITTEE

GRADUATE COLLEGE

UNIVERSITY OF NEBRASKA

ACKNOWLEDGEMENTS

I wish to thank Dr. James D. Carr for his continued interest and assistance throughout the course of this work.

A very special note of thanks is given to my wife, Mary, for her indefatigable patience and understanding, as well as for her assistance, without which the preparation of this dissertation would not have been possible.

Financial assistance from the Environmental Protection Agency, the Nebraska Research Council, and the 3-M Chemical Corporation, is gratefully acknowledged.

TABLE OF CONTENTS

	Page
List of Tables	v
List of Figures	viii
Part I - Dissociation Kinetics of Magnesium	
Aminocarboxylate Complexes	
Introduction	1
Experimental	6
Reagents	6
Apparatus	7
Procedures	9
Results	11
Hydrogen Ion Dependence Studies	11
Ligand Dependence Studies	52
Discussion	73
Intrinsic Dissociation Rate Constants	73
Hydrogen Ion Dependent Dissociation	
Rate Constants	80
Ligand Dependent Rate Constants	85

Part II - Kinetics of the Potassium Ferrate Oxidation Of Certain Nitrogen-containing Compounds, And the Application of Potassium Ferrate to The Determination of Chemical Oxygen Demand	
Introduction	87
Experimental	91
Reagents	91
Apparatus	94
Procedures	101
Results	118
Ferrate Oxidation of Amines	118
Ferrate Oxidation of Ammonia/Ammonium ion	133
Oxygen-evolution Studies	165
COD Measurements	177
Discussion	186
Ferrate Oxidation of Nitrogen-containing Compounds	186
COD Investigation	194
Bibliography	196

LIST OF TABLES

Table		Page
I.	Structures of aminocarboxylate ligands	4
IIa.	Reaction conditions and k_{obs} values for Mg-1-PDTA + CyDTA in the presence of TMAOH	12
IIb.	Reaction conditions and k_{obs} values for Mg-1-PDTA + CyDTA in the prsence of KOH	13
III.	Reaction conditions and k_{obs} values for Mg-d-BDTA + CyDTA in the presence of TMAOH	21
IV.	Reaction conditions and k_{obs} values for MgEDTA + d-CyDTA in the presence of TMAOH	23
V.	Values of the total dissociative and total ligand dependent rate constants for Mg-d-BDTA + CyDTA and MgEDTA + d-CyDTA at the various pH values employed	38

Table	Page
VI. Reaction conditions and k_{obs} values for Mg-m-BDTA + d-CyDTA in the presence of TMAOH	44
VII. Values of resolved rate constants for the various exchange reactions studied	72
VIII. Comparison of dissociative rate constants for alkaline earth aminocarboxylate complexes	74
IX. Formation rate constants of magnesium aminocarboxylate complexes calculated from measured dissociation rate constants	78
X. Extent of proton chelation effect on rate of magnesium complexation with protonated ligands ...	83
XI. Reaction conditions and values of k_{obs} , k_1^{PR} and k_2^{PR} for reactions between potassium ferrate and various amines	119
XII. Comparison of k_2^{PR} values of amine reactions with those of water oxidations	131
XIII. Reaction conditions and k_{obs} values for stoichiometric and excess ferrate reactions with ammonia/ammonium ion	134

Table	Page
XIV. Reaction conditions and values of k_1^{PR} and k_2^{PR} for excess ammonia/ammonium ion reactions	136
XV. Data for k_1^{PR} resolution	147
XVI. Data for k_2^{PR} resolution	153
XVII. Values of resolved rate constants for the reaction of potassium ferrate with ammonia/ammonium ion and various amines	158
XVIII. Comparison of experimental and calculated values of the initial rate for excess total ammonia reactions	159
XIX. Reaction conditions and k_{obs} values for other excess ammonia/ammonium ion reactions	162
XX. Comparison of initial rate values for oxygen-evolution and spectrophotometric reactions	167
XXI. Mass spectral data for the gaseous reaction products of reaction #97	175
XXII. COD values for all wastewater and lake water samples	181

LIST OF FIGURES

Figure		Page
1.	pH profile of the observed psuedo-first-order rate constant for Mg-l-PDTA + CyDTA	15
2.	Hydrogen ion dependence of the observed psuedo-first-order rate constant for Mg-l-PDTA + CyDTA	17
3.	pH profile of the observed psuedo-first-order rate constant for MgEDTA + d-CyDTA	26
4.	pH profile of the observed psuedo-first-order rate constant for MgEDTA + d-CyDTA	28
5.	Hydrogen ion dependence of the observed psuedo-first-order rate constant for Mg-d-BDTA + CyDTA	30
6.	Hydrogen ion dependence of the observed psuedo-first-order rate constant for MgEDTA + d-CyDTA	32

Figure	Page
7. Linear dependence of the observed psuedo-first-order rate constant on excess CyDTA concentration for Mg-d-BDTA + CyDTA	35
8. Resolution of k_H^{MgL} and k_d^{MgL} for Mg-d-BDTA + CyDTA	37
9. Linear dependence of the observed psuedo-first-order rate constant on excess CyDTA concentration for MgEDTA + d-CyDTA	40
10. Resolution of k_H^{MgL} and k_d^{MgL} for MgEDTA + d-CyDTA .	42
11. pH profile of the observed psuedo-first-order rate constant for Mg-meso-EDTA + d-CyDTA	46
12. Hydrogen ion dependence of the observed psuedo-first-order rate constant for Mg-meso-BDTA + d-CyDTA	48
13. pH profile of the observed pseudo-first-order rate constant for Mg-l-PDTA + CyDTA in the presence of KOH	51

14.	First-order hydrogen ion dependence of the total ligand dependent rate constant for Mg-d-BDTA + CyDTA	55
15.	First-order hydrogen ion dependence of the total ligand dependent rate constant for MgEDTA + d-CyDTA	55
16.	Second-order hydrogen ion dependence of the total ligand dependent rate constant for Mg-d-BDTA + CyDTA	57
17.	Second-order hydrogen ion dependence of the total ligand dependent rate constant for MgEDTA + d-CyDTA	59
18.	Resolution of $k_{H_2Cy}^{Mg-d-B}$ and k_{HCy}^{Mg-d-B}	64
19.	Resolution of $k_{H_2Cy}^{MgE}$ and k_{HCy}^{MgE}	66
20.	$k_{Cy_T}/[H^+]$ vs. $1/[H^+]$ for Mg-d-BDTA + CyDTA	69
21.	$k_{Cy_T}/[H^+]$ vs. $1/[H^+]$ for MgEDTA + d-CyDTA	71

Figure	Page
22. Diagram of the steric hinderance present in complexed and uncomplexed forms of EDTA	76
23. Full scale representation of the cell and electrode employed in oxygen-evolution measurements	98
24. pH profile of the general first-order rate constant, k_1^{PR} , for stoichiometric reactions between potassium ferrate and various amines	122
25. Hydrogen ion dependence of k_1^{PR} for stoichiometric diethylamine reactions	124
26. Hydrogen ion dependence of k_1^{PR} for stoichiometric triethylamine reactions.	126
27. Dependence on amine concentration of the observed psuedo-first-order rate constant for reactions employing diethylamine	128
28. Log of the experimental second-order rate constant for water oxidation as a function of pH .	140

Figure	Page
29. Resolution of k_1^{PR} : $k_1^{\text{PR}}/[\text{NH}_3]_0$ vs. $[\text{H}^+]$	144
30. Resolution of k_1^{PR} : $k_1^{\text{PR}}/[\text{NH}_3]_0[\text{H}^+]$ vs. $1/[\text{H}^+]$	146
31. Resolution of k_2^{PR} : $\text{Log } k_{2\text{N}}''$ as a function of pH ..	150
32. Resolution of k_2^{PR} : $\text{Log } k_{2\text{N}}'' + \text{pH}$ vs. $\text{log } C_{\text{NH}_3}$	152
33. Resolution of $k_{2\text{N}}$: $k_{2\text{N}}''/[\text{H}^+][\text{NH}_3]_0^2$ vs. $[\text{H}^+]/[\text{NH}_3]$	157
34. Comparison of the exponential decay curves for identical oxygen-evolution and spectrophotometric reactions	169
35. Arrhenius plot for ammonia/ammonium ion reactions employing varying temperature	173
36. Experimental values of COD as a function of total phenol present	179

PART I

**Dissociation Kinetics of
Magnesium Aminocarboxylate Complexes**

PREVIEW

INTRODUCTION

In the past several years a number of investigations have studied the symmetric, near-symmetric, and enantiomeric exchange reactions of the aminocarboxylate ligands EDTA, PDTA and CyDTA. Structures, names and abbreviations for these ligands are given in Table I. Complexes between these ligands and a variety of metal ions have been used: Calcium (1,2), strontium (3), cadmium (4,5), lead (6,7), nickel (8,9), copper (10), and zinc (11). In the cases of calcium, cadmium, lead and copper, the reactions of all three of these structurally similar ligands have been studied. Only in the cases of calcium and cadmium has the investigation been extended to include the ligand BDPA, a structural intermediate between PDTA and CyDTA. In addition to kinetic studies of this type, the formation of complexes between these ligands and alkali metal ions has also been investigated (12-17).

In many of these studies, dissociative pathways, particularly hydrogen ion catalyzed ones, have been observed in addition to ligand dependent reactions. Certain rate constants for these dissociative pathways for

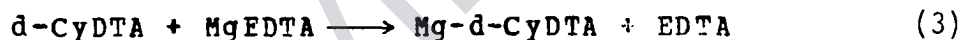
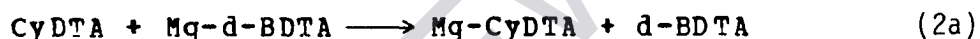
aminocarboxylate complexes of the alkaline earths have been reported (2,3,18-20), but the paucity of information available for the particular member of this family, magnesium, is surprising.

One of the most frequently used techniques for studies of this type has been polarimetry. This of course necessitates the use of an optically active ligand. It further requires that the reaction be slow enough to allow for both mixing of the reactants and response of the mechanical detection system with which most conventional polarimeters are equipped. The rates of the ligand exchange reactions for magnesium aminocarboxylate complexes are such that the polarimetric technique is well suited to their investigation.

The so-called "Eigen mechanism" for the formation reaction of metal ion complexes proposes that the rate-determining step be the loss of water from the primary coordination sphere of the metal ion after the metal ion has formed an outer-sphere complex with the incoming ligand. Accordingly, metal ions may be classified with respect to their rate behavior in the light of this general mechanism. Extensive work of this nature has been carried out for exchange reactions involving monodentate ligands, but only recently have such investigations been extended to multidentate ligands. Included among these have been the

aminocarboxylates (2,21). Although calcium and strontium have been classified in terms of this mechanism, little is known of the corresponding rate behavior of the magnesium ion. The purpose of the present investigation is to provide this information.

In the present study the polarimetric technique was used to measure the kinetics of the following ligand exchange reactions:



From these measurements, dissociative rate constants are determined. These results are then used to calculate formation rate constants through known equilibrium constants and comparisons are made with "Eigen mechanism" formation rate predictions.

TABLE I.

Structures of Aminocarboxylate Ligands

<u>Ligand</u>	<u>Abbreviation</u>
Ethylenediaminetetraacetate	EDTA or Y-4
Structure:	$ \begin{array}{c} \text{OOC-H}_2\text{C} \quad \quad \quad \text{CH}_2\text{-COO}^- \\ \quad \quad \quad \diagdown \quad \quad \diagup \\ \quad \quad \quad \text{N-CH}_2\text{-CH}_2\text{-N} \\ \quad \quad \quad \diagup \quad \quad \diagdown \\ \text{OOC-H}_2\text{C} \quad \quad \quad \text{CH}_2\text{-COO}^- \end{array} $
<u>Ligand</u>	<u>Abbreviation</u>
Propylenediaminetetraacetate	PDTA or P-4
Structure:	$ \begin{array}{c} \text{OOC-H}_2\text{C} \quad \quad \quad \text{CH}_2\text{-COO}^- \\ \quad \quad \quad \diagdown \quad \quad \diagup \\ \quad \quad \quad \text{N-CH-CH}_2\text{-N} \\ \quad \quad \quad \quad \quad \quad \\ \quad \quad \quad \text{CH}_3 \quad \quad \quad \text{CH}_2\text{-COO}^- \\ \text{OOC-H}_2\text{C} \quad \quad \quad \text{CH}_2\text{-COO}^- \end{array} $

TABLE I. Continued

<u>Ligand</u>	<u>Abbreviation</u>
Trans-2,3-Diaminobutane- N,N,N',N'-tetraacetate	BDTA or B-4
Structure:	
<u>Ligand</u>	<u>Abbreviation</u>
Trans-1,2-Diaminocyclohexane- N,N,N',N'-tetraacetate	CyDTA or Cy-4
Structure:	

EXPERIMENTAL

Reagents. All solutions were prepared with deionized, distilled water using standard volumetric glassware. Those used over a period of time as stock solutions were stored in polyethylene bottles. Gilman 2 ml and 0.2 ml microburets were used for all titrations and in preparations of stock solutions and reaction mixtures, where such volumes were appropriate. All pH adjustments were made using reagent grade nitric acid or tetramethylammonium hydroxide (TMAOH - Southwestern Chemicals Inc.). Stock magnesium and zinc ion solutions were prepared from the corresponding reagent grade nitrate salts and standardized by titration with standard disodium EDTA solution. All metal ion-ligand titrations were carried out in excess ammonia buffer (pH~10) using eriochrome black T indicator. Ligand solutions were standardized by titration with either standard magnesium or standard zinc solution. The zinc solution was prepared for use in a separate project not included here. Its use as a standard in this work was bred purely of convenience. The magnesium complexes of each of the various ligands were prepared by mixing stoichiometric amounts of stock magnesium ion solution and the appropriate ligand solution. Stock ligand solutions were prepared from their acids: H_4 EDTA, H_4 -1-PDTA,

H_4 -d-BDTA, H_4 -meso-BDTA, H_4 -d-CyDTA, and H_4 -dl-CyDTA. These ligands had been previously prepared and recrystallized by D. G. Swartzfager (2). The ionic strength of the reaction mixtures was not strictly controlled but varied as follows:

Reaction Mixtures		μ
Mg-l-PDTA	+ 10-fold excess dl-CyDTA	0.3
Mg-l-PDTA	+ > 10-fold excess dl-CyDTA	0.6
Mg-d-BDTA	+ 10-fold excess dl-CyDTA	0.3
Mg-d-BDTA	+ > 10-fold excess dl-CyDTA	0.4 to 1.7*
Mg-meso-BDTA	+ 10-fold excess d-CyDTA	0.08
MgEDTA	+ 10-fold excess d-CyDTA	0.08
MgEDTA	+ > 10-fold excess d-CyDTA	0.1 to 0.14*

* depending upon actual CyDTA concentration

Apparatus. All reactions were monitored polarimetrically with a Perkin-Elmer Model 141 polarimeter equipped with a thermostatted 10 cm cell. A permanent record of optical rotation as a function of time was made by an attached Sargent model SR recorder. All reactions were carried out at $25 \pm 0.2^\circ\text{C}$; such temperature being maintained by a Lauda MGW waterbath. The optical rotations of all but 11 reactions were monitored at 365 nm using the Hg source with which the

polarimeter was equipped. The other 11 reactions (all between MgEDTA and greater than 10-fold excess d-CyDTA) were monitored using an external Bausch and Lomb Xenon source with attached power supply and grating monochrometer. Since these reactions involved a large excess of optically active attacking ligand, the absolute amount of attacking ligand that would be converted to a complexed form would be small. As a result, the observed change in optical rotation (relative to the equilibrium value) would also be small. Since this change in rotation as a function of time is the experimental parameter of real interest, it was hoped that the more intense Xenon source with continuously variable wavelength would maximize its value. After careful alignment of the source with the optics of the polarimeter, the largest optical rotation value for an equilibrium mixture of the reactants of interest occurred at 345 nm. The improvement in signal strength, hence in optical rotation value, was modest: an increase of approximately 50%.

A minimum of 2 hours was required for polarimeter warm-up, after which time signal drift was inconsequential, even for the longest reactions (4 to 6 hours). Prior to every reaction, both the recorder and digital readout were zeroed against an air blank.

Solution pH measurements were made with a Corning model 12 expanded scale pH meter, equipped with standard Corning pH